Available online at www.sciencedirect.com
SCIENCE DIRECT®
International Journal of Mass Spectrometry 228 (2003) 779–795
International Journal of Mass Spectrometry
www.elsevier.com/locate/ijms

Structures and fragmentations of electrosprayed Zn(II) complexes of carboxylic acids in the gas phase Isomerisation versus desolvation during the last desolvation step

Françoise Rogalewicz, Gilles Louazel, Yannik Hoppilliard*, Gilles Ohanessian

Laboratoire des Mécanismes Réactionnels, DCMR, UMR CNRS 7651, Ecole Polytechnique, 91128 Palaiseau Cedex, France

Received 20 February 2003; accepted 31 March 2003

Dedicated to Professor Helmut Schwarz on the occasion of his 60th birthday.

Abstract

Zn^{2+}–carboxylate ions formed in methanol/water solutions are transferred in the gas phase by electrospray. At low cone voltage, species observed in the source spectra correspond to solvated Zn^{2+}–carboxylates: $[RCOOZn, (CH_3OH)_n]^+$ (R = H, CH_3; n = 1–3) ions. Under low energy collisions, all ions with $n > 1$ lose exclusively methanol, mimicking some of the last steps of ion desolvation. However, ions with only one molecule of solvent behave differently: $[HCOOZn, CH_3OH]^+$ eliminates carbon dioxide and $[CH_3COOZn, CH_3OH]^+$ either loses the last molecule of methanol or fragments to give the acylium ion $[CH_3CO]^+$. Labelling experiments as well as accurate molecular orbital calculations are used to explain this different behaviour of $[RCOOZn, CH_3OH]^+$ ions which fragment (totally or partially) instead of losing the last molecule of solvent. It appears that the loss of the last molecule of solvent from $[HCOOZn, CH_3OH]^+$ requires more energy than does its isomerisation into $[CO_2, HZn, CH_3OH]^+$, precursor for the loss of CO_2. For $[CH_3COOZn, CH_3OH]^+$, isomerisation processes and direct loss of methanol require very similar energies. In both cases, part of the gaseous ions formed after complete desolvation are chemically different from their precursors in solution.

Keywords: Mass spectrometry; Electrospray; Zinc complexes; Carboxylic acids; Desolvation; Quantum calculations

1. Introduction

The common wisdom that electrospray ionisation is a gentle process which produces gas phase ions which are faithful images of their solution phase precursors does not apply to certain categories of metal ions.

Metal ions embedded in a large number of solvent molecules have small desolvation energies, so that stepwise desolvation is by far the lowest energy process. When solvent molecules get fewer, and especially when all are in the first coordination sphere of the metal ion, desolvation energies rise sharply. For instance, dehydration enthalpies at 298 K

* Corresponding author. Tel.: +33-1-69-33-34-04; fax: +33-1-69-33-30-41.
E-mail address: yannik.hoppilliard@polytechnique.fr (Y. Hoppilliard).

1387-3806/$ – see front matter © 2003 Elsevier B.V. All rights reserved.
doi:10.1016/S1387-3806(03)00244-6

of $Zn^{2+}(H_2O)_n$ to $Zn^{2+}(H_2O)_{n-1}$ plus H_2O remain lower than 105 kJ/mol for $n \geq 4$, and then rise to 179 and 233 when n decreases to 4 and 3. With $n = 2$ and 1, dehydration energies reach values dramatically high (368 and 431 kJ/mol, respectively). With such large energies required, other processes may start to compete with simple desolvation [1,2].

In a previous paper [3], we have shown that the evaporation of the last molecule of methanol bound to $[CH_3OZn]^+$ requires a dissociation energy of 261 kJ/mol. From $[Gly\text{-}H + Zn]^+$, this enthalpy is calculated to be 186, 218 and 263 kJ/mol for the following molecules of solvent: H_2O, CH_3OH and CH_3CN, respectively [6]. These energies are large enough that there exist structural rearrangements requiring less energy than desolvation. Such rearrangements lead to fully desolvated gaseous ions having a structure which may be different from that of their condensed phase precursors, contrary to what is generally expected for electrosprayed ions. In fact, a mixture of isomers may be formed. Such rearrangements were shown to occur in the zinc complex of methanol $[CH_3OZn, CH_3OH]^+$ [3] isomerising into $[CH_2O, HZn, CH_3OH]^+$ and the zinc complex of the simplest amino acid, glycine: $[Gly\text{-}H + Zn, CH_3OH]^+$, in which three different isomerisations were identified [4,5].

In this paper, we have investigated the decomposition processes of $[HCOOZn, (CH_3OH)_n]^+$ and $[CH_3COOZn, (CH_3OH)_n]^+$. As compared to glycine, small aliphatic carboxylic acids lack the amino group and are therefore expected to be prone to less many low-energy rearrangements. The question therefore arises: are there still rearrangements which may compete with direct desolvation?

Mass spectrometric experiments were carried out to determine the gas phase behaviour of the Zn^{2+}–carboxylate complexes of formic and acetic acids micro-solvated with one to three molecules of methanol. Collisional activation as well as deuterium labelling were used to probe ion structures. Fragmentation pathways were determined with ab initio calculations, providing a complete picture of the competition between metal carboxylate isomerisation and solvent elimination.

2. Experimental and computational

2.1. Experimental

Electrosprayed Zn^{2+}–carboxylate complexes of various carboxylic acids, RCOOH, were formed from a RCOOH/$ZnCl_2$ mixture (1 mM and 500 μM, respectively) in 50:50 v/v solutions of water/methanol. Solutions were infused in the ion source with a syringe pump (Harvard, Southnatic, MA, USA) at a flow rate of 10 μL/min. Formic and acetic acids were purchased from Aldrich Chem. Co. (Saint Quentin Fallavier, France) and anhydrous $ZnCl_2$ was obtained from Merck KGaA (Darmstadt, Germany). All solvents were of HPLC grade.

All experiments were carried out on a triple quadrupole Quattro II mass spectrometer (Micromass, Manchester, UK). Source parameters were adjusted so as to optimize ion signals such as $[RCOOH\text{–}H + Zn, CH_3OH]^+$. Typical voltage values were: capillary 2.5–3.5 kV, counter electrode 0.1–0.3 kV, RF lens 0.7 eV, skimmer 1.5 V, cone voltage 10–40 V.

Low energy collision-induced dissociation (CID) of $[RCOOH\text{–}H + Zn, (CH_3OH)_n]^+$ and their fragments were performed with argon as the collision gas (at a pressure of 7.5×10^{-4} mbar in the collision cell). The decomposition of $[RCOOH\text{–}H + Zn, CH_3OH]^+$ was studied as a function of collision energy in the laboratory frame (E_{lab}), typically in the 0–24 eV range. The results are presented as breakdown graphs showing the abundances of the various fragment ions as a function of collision energy. The gas pressure used is high enough to allow for multiple collisions, so that the energies imparted to the ions may be higher than the collision energies indicated. Therefore, no attempt was made to relate the absolute collision energies to the computed critical energies of the various fragmentations. All CID experiments were preceded by mass selection of the isotopomer of $[RCOOH\text{–}H + Zn, CH_3OH]^+$ involving ^{64}Zn. Each m/z ratio indicated in the text for ions containing zinc corresponds to the ^{64}Zn isotope.

2.2. Computational

As in our previous work [3–6], two basis sets were used in this study. For geometry optimizations and vibrational frequency calculations, the 6-31G* basis set was used for H, C, N and O, and the Wachters [14s9p5d1f/9s5p3d1f] was used for Zn [7]. This is referred to as basis1. For final energy calculations, basis2 consists in the 6-311+G(2d,2p) for H, C, N and O, and the extended Wachters basis [15s11p6d2f/10s7p4d2f] for Zn [7]. Geometry optimizations and vibrational frequency calculations were carried out at the HF/basis1 level. These calculations were also used to obtain thermal corrections at 298 K (E_{therm}). No special treatment was applied to correct for the larger relative errors on small frequencies computed in the harmonic approximation. Extensive tests [3–6] showed that the use of HF rather than MP2 geometries leads to very small errors in final energy calculations. Final energetics were obtained with MP2(FC)/basis2 wavefunctions at the HF/basis1 geometries, a level denoted below as MP2(FC)/basis2//HF/basis1 (where FC indicates that the frozen core approximation was applied to the 1s electrons of C, N and O and to the 1s, 2s, and 2p electrons of Zn). The Gaussian98 program package [8] was used throughout. In the text, the relative energies are always given at the best level of theory (MP2(FC)/basis2//HF/basis1) and include the thermal corrections at 298 K performed at the HF/basis1 level.

3. Results and discussion

In the whole range of experimental conditions used, all ions observed are singly charged, resulting from deprotonation of one of the organic ligands by Zn^{2+}. Since the acidities of HCO_2H and CH_3CO_2H are much larger than that of CH_3OH, it is expected that the ions observed are of the form $[RCO_2Zn, (CH_3OH)_n]^+$ rather than $[RCO_2H, CH_3OZn, (CH_3OH)_{n-1}]^+$ (R = H, CH_3), i.e., a zinc-bound carboxylate ion microsolvated by a varying number, *n*, of methanol molecules.

3.1. Zn(II)–acid formic complexes solvated by methanol: $[HCOOZn, (CH_3OH)_n]^+$

At cone voltage values in the 10–40 V range, the source spectra recorded by scanning the first quadrupole indicate the dominant formation of $[HCOOZn, (CH_3OH)_n]^+$ (n = 1–3), with n decreasing with increasing cone voltage. For n = 1, this ion is called **1**. Low energy collisions of the selected *m/z* 173 ions, $[HCOOZn, (CH_3OH)_2]^+$ termed hereafter [**1**, CH_3OH], exclusively produce **1**, $[HCOOZn, CH_3OH]^+$ (*m/z* 141). This corresponds to a loss of methanol, mimicking the second to last step of desolvation of $HCOOZn^+$. In contrast with this expected result, low energy collisions of **1** produce $HCOOZn^+$ (*m/z* 109) in only minor amounts, while the main process observed is the loss of CO_2 at *m/z* 97 (Fig. 1).

In order to provide a rationale for these observations, potential energy profiles associated with the low energy fragmentations of both [**1**, CH_3OH] and **1** were calculated.

3.1.1. The $[HCOOZn, (CH_3OH)_2]^+$ system

Concerning the $[HCOOZn, (CH_3OH)_2]^+$ system, the geometries of three structures were calculated and are presented in Fig. 2: the formate complex, [**1**, CH_3OH]; the rearranged form $[CO_2, HZn, (CH_3OH)_2]^+$ allowing loss of CO_2 and termed [**2**, CH_3OH]; and the transition state TS [**1**, CH_3OH] [**2**, CH_3OH] connecting these two isomeric minima. The energies associated with these various structures and with the fragmentation leading to **1** by loss of methanol are given in Table 1. It appears, as expected, that the direct loss of methanol requires less energy (137 kJ/mol) than does the isomerisation of [**1**, CH_3OH] into [**2**, CH_3OH] (transition state located 157 kJ/mol above [**1**, CH_3OH]). Therefore, when $HCOOZn^+$ is solvated with two methanol molecules, isomerisation into $[CO_2, ZnH, (CH_3OH)_2]^+$ cannot compete with methanol elimination (see Fig. 3).

3.1.2. The $[HCOOZn, CH_3OH]^+$ system

As seen before, at low collision energies (E_{lab} < 8 eV), the $[HCOOZn, CH_3OH]^+$ ion, formed by

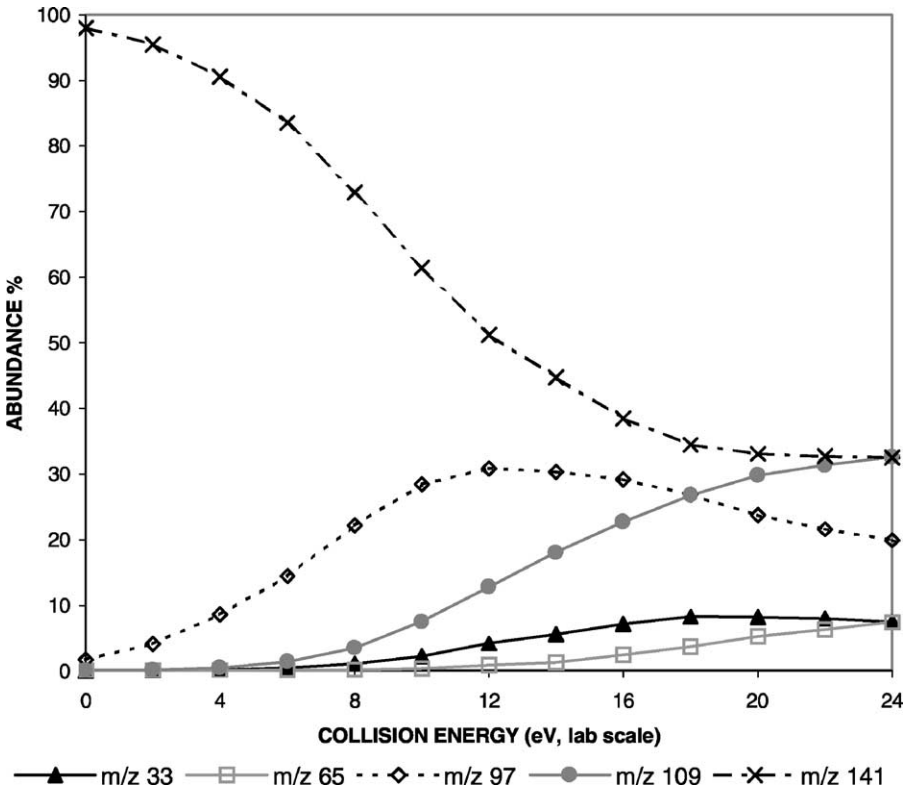

Fig. 1. Breakdown graph associated with the decomposition of [HCOOZn, CH_3OH]$^+$ (*m*/*z* 141), i.e., loss of methanol (*m*/*z* 109); loss of carbon dioxide (*m*/*z* 97); formation of ZnH^+(*m*/*z* 65); formation of $CH_3OH_2{}^+$ (*m*/*z* 33).

elimination of methanol from [**1**, CH_3OH], eliminates competitively CH_3OH and CO_2, the latter being greatly favoured. With increasing values of the collision energy, the relative intensities of the two fragmentations change to the extent that loss of methanol becomes dominant (above $E_{lab} = 18$ eV). Moreover, above 10 eV, minor peaks corresponding to the formation $CH_3OH_2{}^+$ and HZn^+ are also observed, but with very low intensities at all collision energies.

Elimination of methanol (32 u) is the only decomposition expected from **1**. Given the very high energy demand for this direct process (247 kJ/mol, vide infra), these experimental results suggest that all fragmentations observed at low collision energies involve

Table 1
Total energies, *E* (MP2(FC)/basis2//HF/basis1), thermal corrections at 298 K, E_{therm} (HF/basis1) and relative $\Delta(E + E_{therm})$ enthalpies derived from these results for the [HCOOZn, $(CH_3OH)_2$]$^+$ system

Ions	*E* (Hartree)	E_{therm} (kJ/mol)	$\Delta(E + E_{therm})$ (kJ/mol)
[**1**, CH_3OH]	−**2198.106000**	406	0
[**2**, CH_3OH]	−2198.089033	391	30
TS [**1**, CH_3OH]–[**2**, CH_3OH]	−2198.039380	388	157
1 + CH_3OH	−2198.050042	396	137

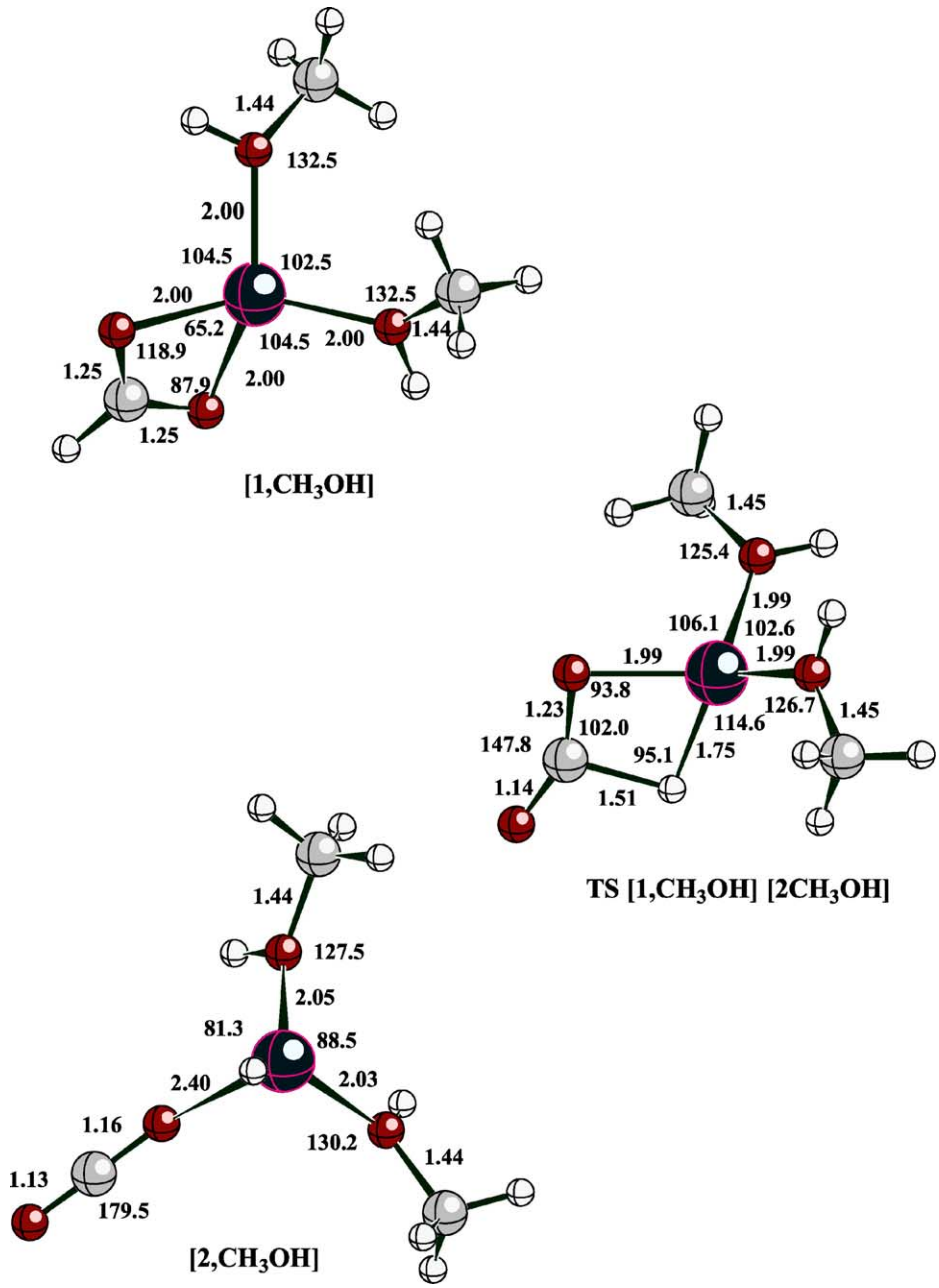

Fig. 2. Geometries of isomers [**1**, CH_3OH] and [**2**, CH_3OH] and of transition state TS [**1**, CH_3OH] [**2**, CH_3OH] (bond lengths in Å, angles in degrees).

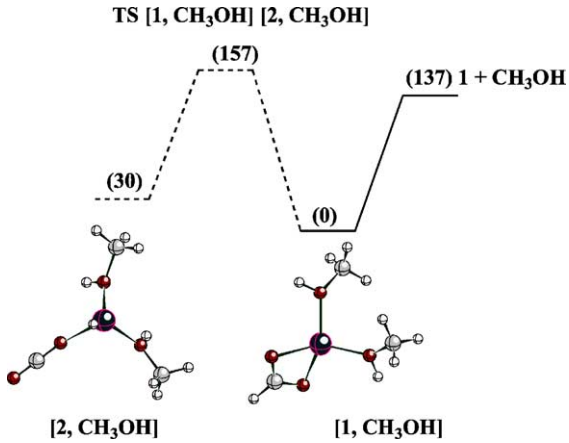

Fig. 3. Potential energy profile of the [HCOOZn, $(CH_3OH)_2]^+$ system. Relative energies (in kJ/mol) are given in parenthesis.

rearrangements of **1** prior to dissociation. In order to provide a rationale for these observations, several isomerisation processes of **1** were investigated.

The computed geometries associated with various isomeric structures and transition states connecting these minima are given in Fig. 4 while the relative energies of the various states are listed in Table 2. The potential energy profile associated with the isomerisations and fragmentations of **1** is presented in Fig. 5.

Loss of carbon dioxide requires the isomerisation of **1** into a structure in which the metal ion is in interaction with carbon dioxide. Such a structure, [CO_2, ZnH, $CH_3OH]^+$, called **2**, is obtained by β-hydrogen transfer from the formate to the zinc ion. The rate limiting step (transition state) of this isomerisation is located 169 kJ/mol above **1** (taken as the reference energy) while the direct elimination of methanol from **1** requires 247 kJ/mol. Consequently, the isomerisation is energetically much more favourable. Moreover, methanol and carbon dioxide may be competitively eliminated from the rearranged structure **2**. The most stable final state associated with these fragmentations, [HZn, $CH_3OH]^+ + CO_2$, is located 37 kJ/mol above **1**, while the elimination of methanol is close in energy to the transition state TS **1**–**2** (157 kJ/mol vs. 169 kJ/mol above **1**, respectively).

At high collision energy the ion [HZn, $CH_3OH]^+$ formed by CO_2 elimination from **2** either may lose CH_3OH to give HZn^+ or rearrange to form protonated methanol by loss of reduced zinc (see Fig. 5 and

Table 2
Total energies, E (MP2(FC)/basis2//HF/basis1), thermal corrections at 298 K, E_{therm} (HF/basis1) and relative $\Delta(E + E_{therm})$ enthalpies derived from these results for the $[HCO_2Zn, CH_3OH]^+$ system

Ions	E (Hartree)	E_{therm} (kJ/mol)	$\Delta(E + E_{therm})$ (kJ/mol)
$[HCOOZn, CH_3OH]^+$ **1**	**−2082.574431**	242	0
$[HZn, CO_2, CH_3OH]^+$ **2**	−2082.567778	229	4
$[CH_3OZn, HCO_2H]^+$ **3**	−2082.546052	242	75
$[HZn^+, HCO_2H, OCH_2]^+$ **4**	−2082.541557	226	70
TS **1**–**2**	−2082.503531	225	169
TS **1**–**3**	−2082.537501	228	83
TS **3**–**4**	−2082.484107	224	219
$[HCO_2Zn]^+ + CH_3OH$	−2082.476348	232	247
$[HZn, CO_2]^+ + CH_3OH$	−2082.506309	220	157
$[HZn, CH_3OH]^+ + CO_2$	−2082.552017	220	37
$CH_3OZn^+ + HCO_2H$	−2082.447946	232	322
$HZn^+(OCH_2) + HCO_2H$	−2082.493382	218	189
$HZn^+(HCO_2H) + OCH_2$	−2080.644671	218	165
$HZn^+ + CO_2 + CH_3OH$	−2082.457782	212	276
TS $[HZn, CH_3OH]^+$	−2082.477552	216	228
$[CH_3OH_2, Zn^\circ]^+ + CO_2$	−2082.522848	236	130
$CH_3OH_2^+ + CO_2 + Zn^\circ$	−2082.506891	233	169

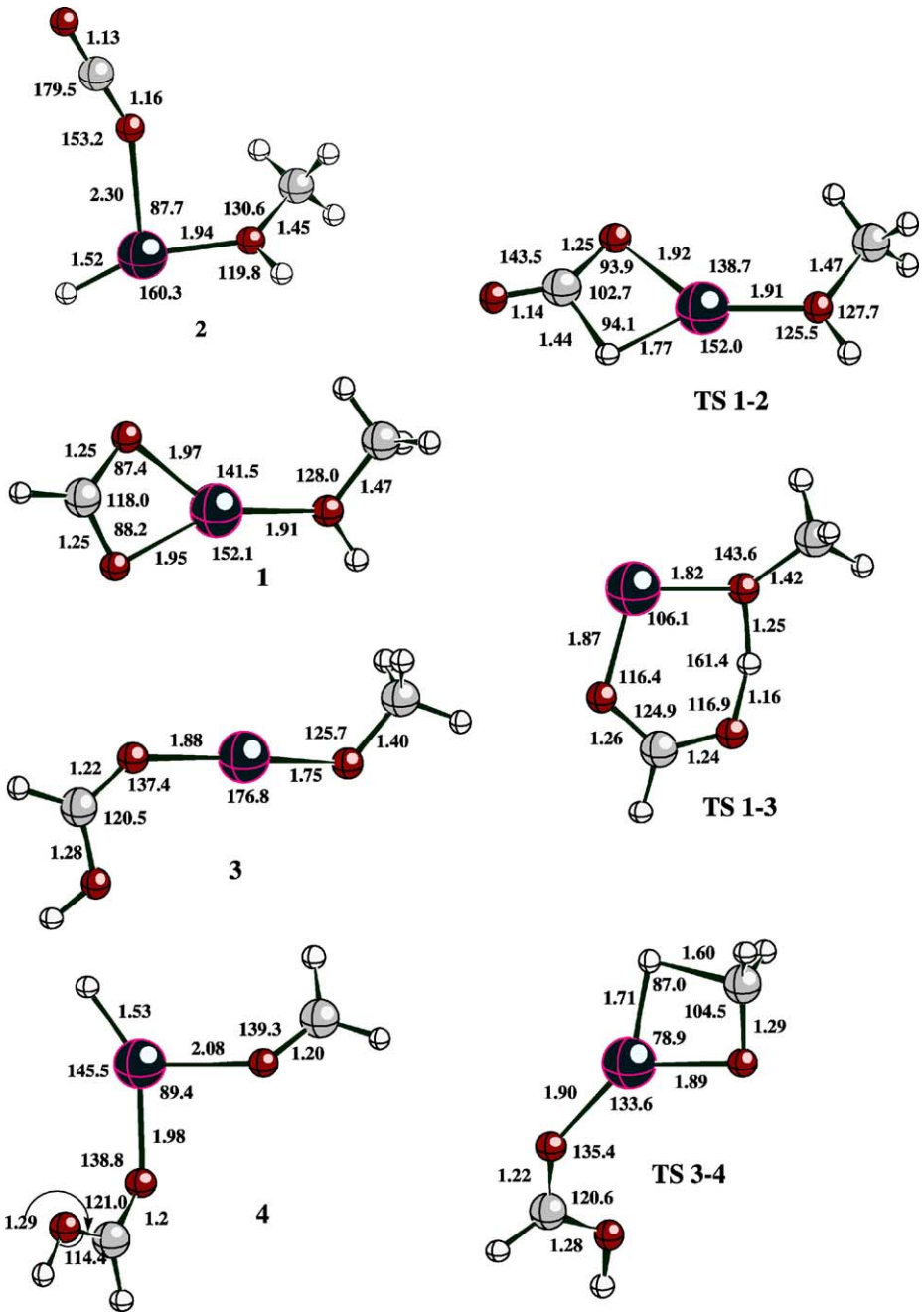

Fig. 4. Geometries of isomers **1**, **2**, **3**, **4** and of transition states TS **1**–**2**, TS **1**–**3** and TS **3**–**4** (bond lengths in Å, angles in degrees).

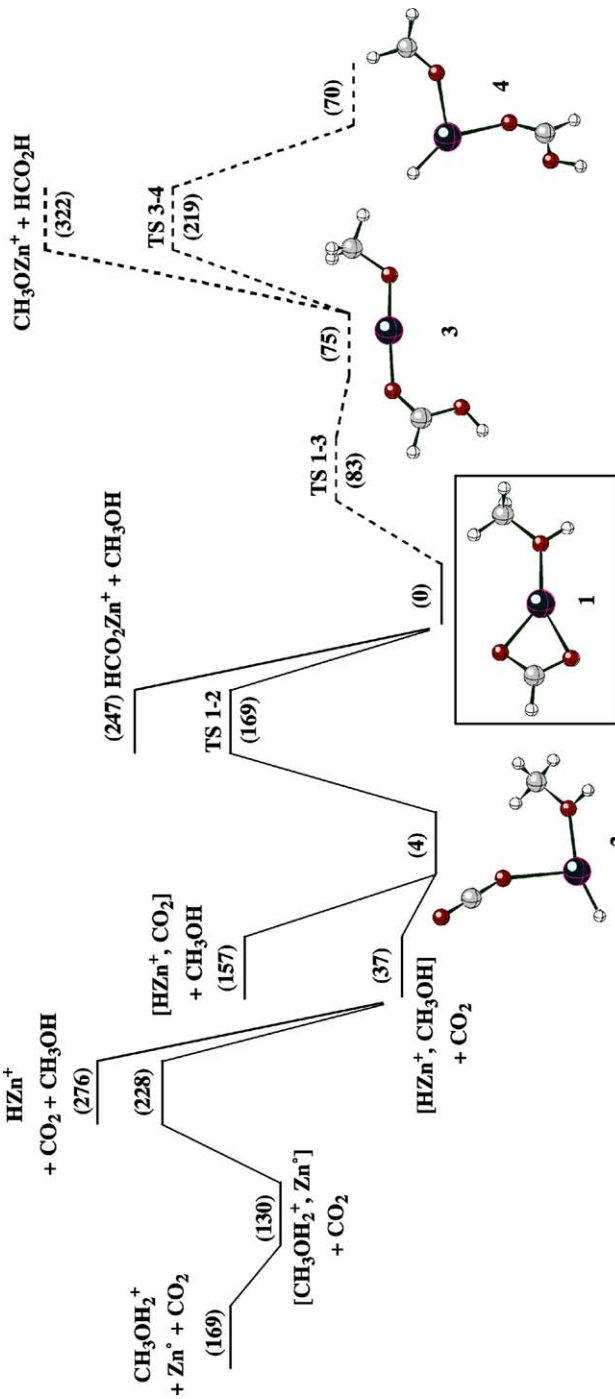

Fig. 5. Potential energy profile of the $[HCOOZn, CH_3OH]^+$ system. Relative energies (in kJ/mol) are given in parenthesis.

Table 2). This would account for the marginal formations of both ions.

Although the above results provide a consistent description of the fragmentations observed, another type of isomerisation of **1** was considered. Our previous work on the analogous ion [Gly-H+Zn, CH_3OH]$^+$ (in which formic acid is replaced by glycine) led us to suspect that the isomeric form **3** [HCOOH, $ZnOCH_3$]$^+$ might also be quite stable. It turned out that it is not the case, since **3** is computed to lie 75 kJ/mol higher than **1** (see Table 2 and Fig. 5). Forming **3** from **1** requires acidic proton transfer from the methanol to the formate, whose activation barrier is 83 kJ/mol. Direct elimination of formic acid from **3** yields a final state CH_3OZn^+ + HCOOH at 322 kJ/mol, much too high for CH_3OZn^+ (*m*/*z* 95) to be formed. From **3**, a classical β-H transfer finally would yield the 3-ligand complex [HCOOH, ZnH, CH_2O]$^+$, **4**, able to lose HCOOH and H_2CO competitively leading to final states located at 189 and 165 kJ/mol above **1**, respectively. However, the transition state for β-H transfer is high in energy, 219 kJ/mol, so that this pathway cannot compete with isomerisation of **1** into **2**: the rate-limiting barrier of the latter is 50 kJ/mol more favourable.

From these results, a scenario emerges which is in full agreement with the experimental observations: at low collision energies, the most favourable process involves isomerisation of **1** into **2**, followed by loss of CO_2 (major) or CH_3OH (minor). At still higher energies, direct elimination of CH_3OH from **1** becomes possible. This simple bond breaking being dynamically favoured over multi-step rearrangements, it takes over and loss of CH_3OH eventually becomes dominant.

3.2. [CH_3COOZn, CH_3OH]$^+$

Fig. 6 gives the breakdown graph associated with the fragmentations of [CH_3CO_2Zn, CH_3OH]$^+$ (*m*/*z* 155, named **5** hereafter) as a function of collision energy. Four fragmentations appear on this graph, two are prominent (loss of methanol at *m*/*z* 123 and formation of CH_3CO^+ at *m*/*z* 43) and two remain of low abundance at all energies (losses of ketene at *m*/*z* 113 and of water at *m*/*z* 137).

Labelling experiments were carried out, using either CD_3OH as solvent, or CD_3CO_2H as reagent or a mixture of CH_3OD and CH_3CO_2D (solvent and reagent, respectively). The various parent ions formed during these experiments were dissociated under low energy collisions in order to reveal the origin of the hydrogen atoms involved in each fragment ion. The ions formed as well as the molecules lost during these dissociations (E_{lab} = 18 eV) are presented in Table 3.

The optimized geometries of the species (minima and transition states) involved in these profiles are given in Figs. 7 and 9. The potential energy profiles associated with the formation of the observed fragments are presented in Figs. 8 and 10. The relative energies of initial, intermediate, transition and final states are gathered in Table 4.

In the following sections, we describe the mechanisms and energetics of the four fragmentations observed, and finally put the results together to obtain a consistent description of the dissociation of **5**.

3.2.1. Loss of methanol

Table 3 shows that for the greatest part, the methanol molecule lost from labelled parent ions is the solvent molecule. The simplest way to account for this observation is a direct detachment of methanol from [CH_3CO_2Zn, CH_3OH]$^+$. This process is computed to require 239 kJ/mol (Table 4, Fig. 8). However, for a smaller part, [CD_3CO_2Zn, CH_3OH]$^+$ and [CH_3CO_2Zn, CH_3OD]$^+$ lose a molecule of methanol including a hydrogen atom coming from the methyl group of the acetate. The prerequisite for such a loss is an isomerisation of the parent ion which will be described together with the loss of ketene and demonstrated to be more energy demanding than the direct loss of methanol.

3.2.2. Formation of the acylium ion

The formation of the acylium ion CH_3CO^+ at *m*/*z* 43 involves exclusively the methyl group of the acetate function (see Table 3). Two decomposition processes

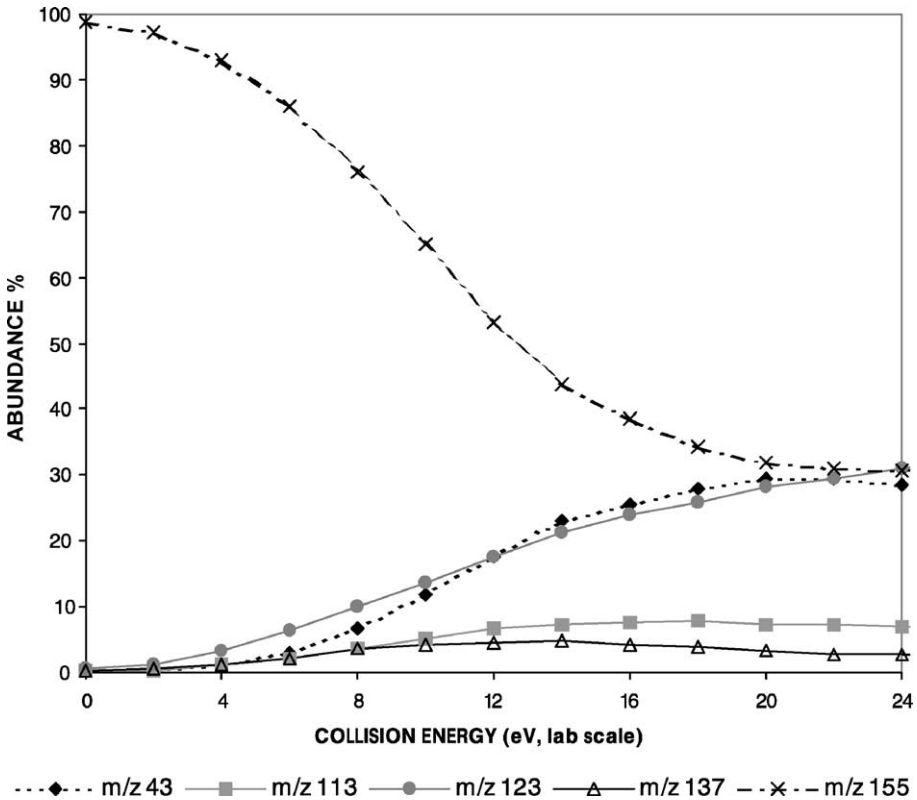

Fig. 6. Breakdown graph for the fragmentations of $[CH_3COOZn, CH_3OH]^+$ (*m*/*z* 155), i.e., *m*/*z* 43: formation of CH_3CO^+; *m*/*z* 113: loss of ketene; *m*/*z* 123: loss of methanol; *m*/*z* 137: loss of water.

yielding CH_3CO^+ were investigated and are presented in Scheme 1.

Mechanism (A) involves the neutralization of the zinc atom, in the $[CH_3CO_2Zn, CH_3OH]^+$ ion **5**, to form either via an ion/neutral complex intermediate or in one step the acylium ion and the complex (ZnO, CH_3OH). The energy of this final state is dramatically high (498 kJ/mol) so that this process can be definitively excluded.

The second mechanism (B), first requires transfer of the acidic proton of methanol to the acetate, to form isomer **6** $[CH_3CO_2H, ZnOCH_3]^+$. From **6**, this mechanism associates the formation of acylium and the elimination of $HOZnOCH_3$. There are two conformers

Table 3
Decomposition under collision (E_{lab} = 18 eV) of $[CX_3COOZn, CX_3OX]^+$ (X = H or D)

Parent ion	Loss of water	Loss of methanol	Loss of ketene	Loss of CH_3OZnOH
$[CH_3COOZn, CH_3OH]^+$ (*m*/*z* 155)	$-H_2O$ (*m*/*z* 137)	CH_3OH (*m*/*z* 123)	$-CH_2CO$ (*m*/*z* 113)	$-CH_3OZnOH$ (*m*/*z* 43)
$[CH_3COOZn, CD_3OH]^+$ (*m*/*z* 158)	$-H_2O$ (*m*/*z* 140)	$-CD_3OH$ (*m*/*z* 123)	$-CH_2CO$ (*m*/*z* 116)	$-CD_3OZnOH$ (*m*/*z* 43)
$[CD_3COOZn, CH_3OH]^+$ (*m*/*z* 158)	–HDO (*m*/*z* 139)	$-CH_3OH$ (*m*/*z* 126) 69% $-CH_3OD$ (*m*/*z* 125) 31%	$-CD_2CO$ (*m*/*z* 114)	$-CH_3OZnOH$ (*m*/*z* 46)
$[CH_3COOZn, CH_3OD]^+$ (*m*/*z* 156)	–HDO (*m*/*z* 137)	$-CH_3OH$ (*m*/*z* 124) 24% $-CH_3OD$ (*m*/*z* 123) 76%	$-CH_2CO$ (*m*/*z* 114)	$-CH_3OZnOD$ (*m*/*z* 43)

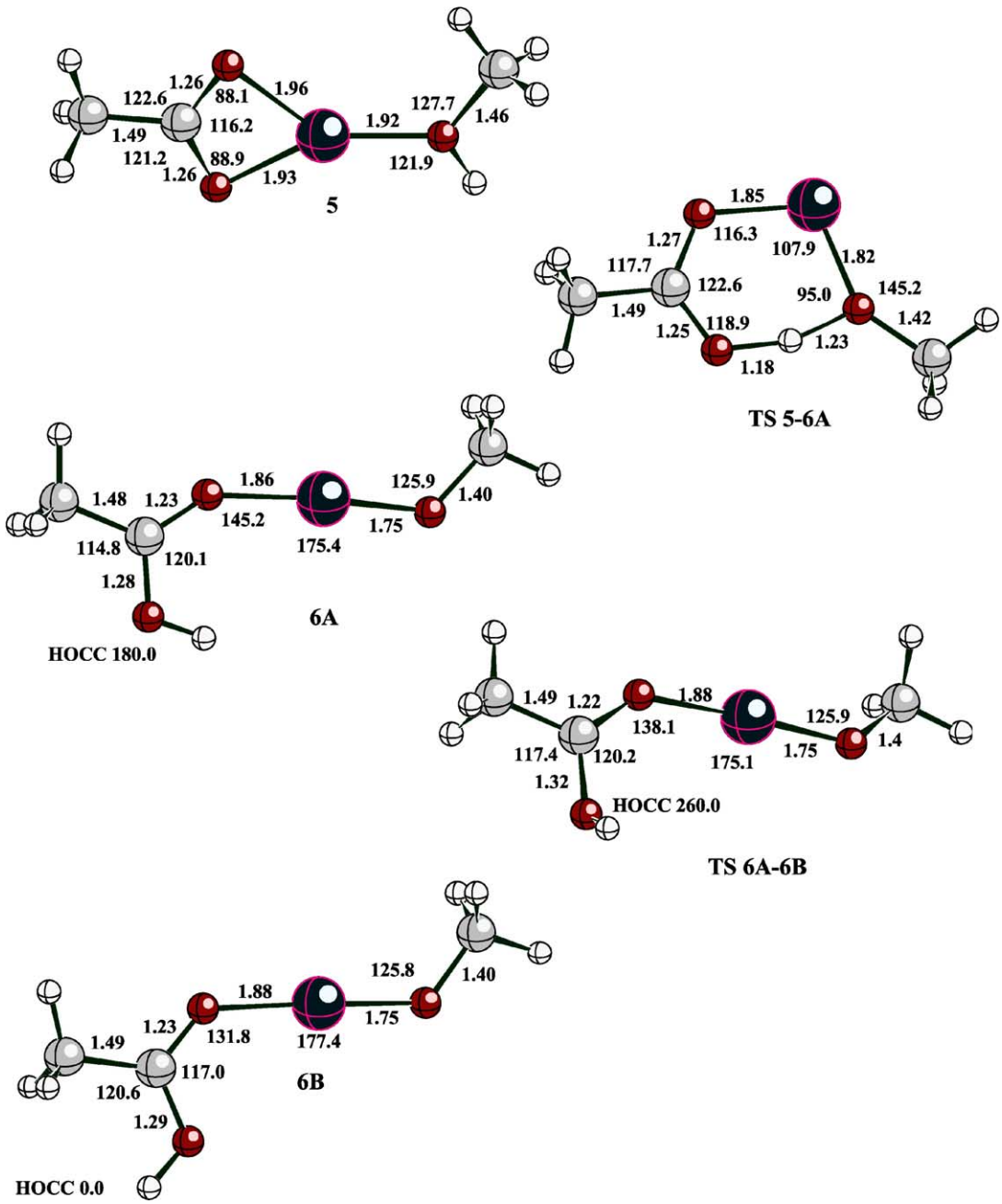

Fig. 7. Geometries of isomers **5**, **6A** and **6B** and of transition states TS **5**–**6A** and TS **6A**–**6B** (bond lengths in Å, angles in degrees).

of $[CH_3CO_2H, ZnOCH_3]^+$, **6A** and **6B**, differing by the orientation of the hydroxylic hydrogen in the acetic acid molecule and very close together in energy (72 and 65 kJ/mol, respectively, above **5**) (see Figs. 7 and 8 and Table 4). Transfer of the labile hydrogen from methanol to acetate requires few activation energy (83 kJ/mol) and leads to **6A**. However, **6B** is a better precursor than **6A** for the hydroxyl group transfer on

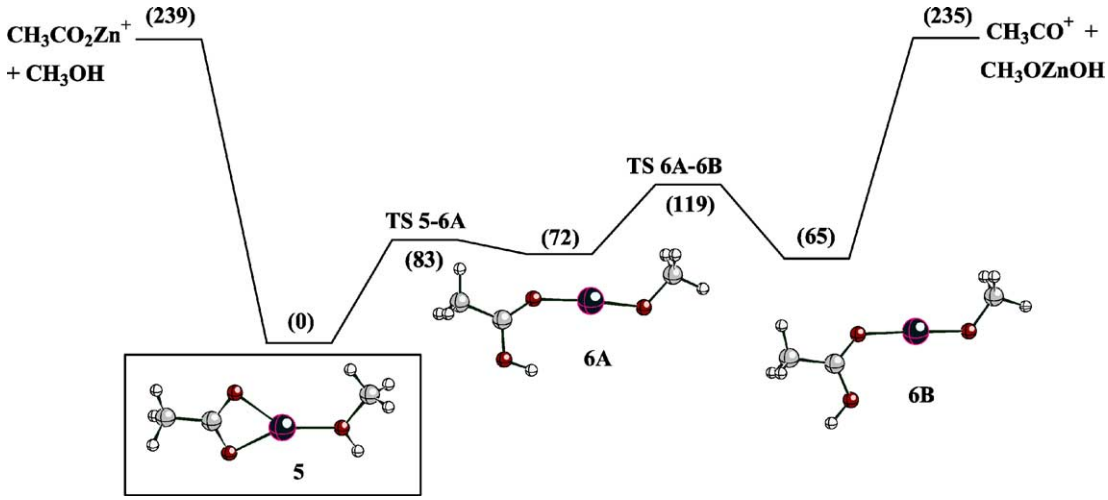

Fig. 8. Potential energy profile of the $[CH_3COOZn, CH_3OH]^+$ system. Direct loss of methanol vs. isomerisation leading to formation of acylium CH_3CO^+. Relative energies (in kJ/mol) are given in parenthesis.

the zinc atom. The transition state for the interconversion (TS **6A–6B**) is located 119 kJ/mol above **5**.

The potential energy surface was extensively explored in order to locate a transition state corresponding to hydroxyl transfer from the acetic acid onto zinc. No such structure could be located. This exploration showed that there is a continuous increase in energy from structure **6B** to the dissociation

Table 4
Total energies, E (MP2(FC)/basis2//HF/basis1), thermal corrections at 298 K, E_{therm} (HF/basis1) and relative $\Delta(E + E_{therm})$ enthalpies derived from these results for the $[H_3CCO_2Zn, CH_3OH]^+$ system (initial, intermediates, transition and final states)

Ions	E (Hartree)	E_{therm} (kJ/mol)	$\Delta(E + E_{therm})$ (kJ/mol)
$[H_3CCO_2Zn, CH_3OH]^+$ **5**	**−2121.798657**	323	0
$[CH_3OZn, H_3CCO_2H]^+$ **6A**	−2121.771388	323	72
$[CH_3OZn, H_3CCO_2H]^+$ **6B**	−2121.774025	323	65
$[CH_3OZn, H_2CCO, H_2O]^+$ **7**	−2121.727411	308	171
$[CH_2{=}C(OH)OZn, CH_3OH]^+$ **8**	−2121.737657	321	158
$[HOZn, CH_3OH, CH_2CO]^+$ **9**	−2121.739890	312	143
TS **5–6A**	−2121.761598	309	83
TS **6A–6B**	−2121.750804	316	119
TS **6B–7**	−2121.723376	298	172
TS **7–9**	−2121.703996	299	224
TS **6B–8**	−2121.703724	308	234
TS **8–9**	−2121.720031	311	194
$H_3CCO_2Zn^+ + CH_3OH$	−2121.704173	314	239
$H_3CCO^+ + (ZnO, CH_3OH)$	−2121.601877	304	498
$H_3CCO^+ + CH_3OZnOH$	−2121.702170	305	235
$H_3CCO^+ + (H_2CO, Zn, H_2O)$	−2119.616579	305	354
$[H_3COZn, H_2O]^+ + CH_2{=}C{=}O$	−2121.694762	304	254
$[H_3COZn, CH_2{=}C{=}O]^+ + H_2O$	−2121.677487	302	297
$[HOZn, CH_3OH]^+ + CH_2{=}C{=}O$	−2121.707589	305	221
$[HOZn, CH_2{=}C{=}O]^+ + CH_3OH$	−2121.677166	303	299
$H_2C{=}C(OH)OZn^+ + CH_3OH$	−2121.640970	311	402

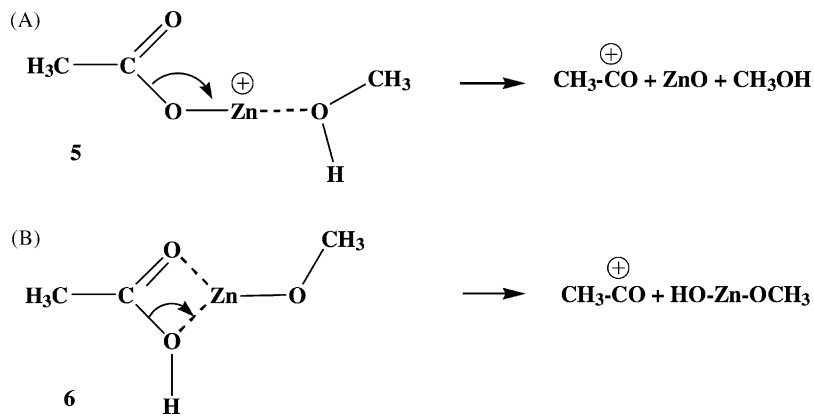

Scheme 1.

products CH_3CO^+ and $HOZnOCH_3$. Therefore, the critical energy for this process is that of the exit channel, 235 kJ/mol. Another combination of products is CH_3CO^+ and $H_2OZnOCH_2$, it is found to lie 354 kJ/mol above **5** and therefore cannot be competitive.

3.2.3. Loss of water

Table 3 shows that the loss of water involves the acidic hydrogen (loss of HDO from $[CH_3CO_2Zn, CH_3OD]^+$) and a hydrogen of the methyl group of the carboxylate function (loss of HDO from $[CD_3CO_2Zn, CH_3OH]^+$). According to these results, an intermediate **7** in which the ion CH_3OZn^+ is in interaction with water and ketene is a good precursor for water elimination. **7** arises from **6B** in two steps: hydroxyl migration to zinc, and migration of a hydrogen atom from the acetate methyl group to the hydroxyl (Figs. 9 and 10). It has been shown earlier (vide supra formation of CH_3CO^+) that there is not transition state associated with the first step (C–O(H) breaking). In the present case, the cleavage of C–O(H) is assisted by the hydrogen transfer leading straight to **7**.

The transition state TS **6B**–**7** and the intermediate **7** are very close together in energy (172 and 171 kJ/mol above **5**, respectively). The decomposition of **7** leads competitively to loss of ketene or water located 254 and 297 kJ/mol above **5**, respectively.

3.2.4. Loss of ketene

The ketene molecule which is eliminated is expected to arise from the fragmentation of the acetate ligand. Labelling experiments confirm the assumption. It has been shown, just before, that the intermediate **7** is an appropriate precursor not only for the loss of water but also for that of ketene. Moreover, it is to be noticed that, from **7**, ketene loss is easier than water loss (vide supra). A second suitable precursor for ketene elimination is an intermediate **9** in which the ion $HOZn^+$ is in interaction with methanol and ketene allowing the competitive elimination of both molecules.

In Scheme 2, two mechanisms are proposed to explain the formation of **9**. Both mechanisms start from **6B**, which is easily formed from **5**, and lead to **9** via **7** or **8**.

The isomerisation of **6B** into **7** has been described before. From **7**, hydrogen transfer from the water molecule to the oxygen of methanolate leads to **9**. The transition state TS **7**–**9**, located 224 kJ/mol above **5**, is the rate limiting step for the isomerisation of **5** into **9**.

The second pathway involves, to isomerise **6B** into **8**, a 1–5 hydrogen transfer from the methyl of the acetate group to the oxygen atom of the methylate group. This migration is followed by the hydroxyl transfer on the zinc ion to yield $[CH_2{=}C{=}O, HOZn, CH_3OH]^+$, **9**. The rate limiting barrier of the reaction leading from **6B** to **9** via **8** is TS **6B**–**8**, located

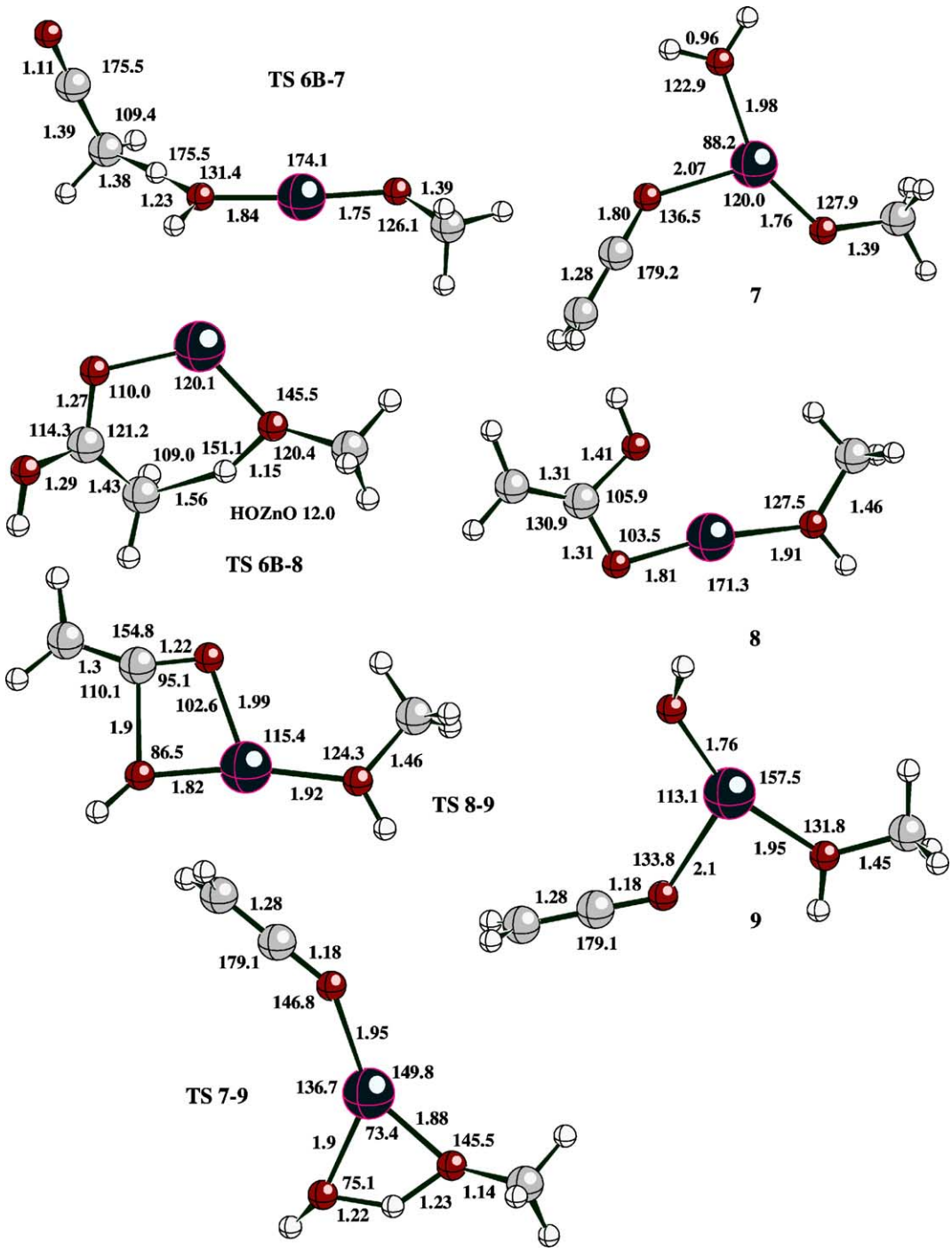

Fig. 9. Geometries of isomers **7**, **8**, **9** and of transition states TS **6B**–**7**, TS **6B**–**8**, TS **7**–**9** and TS **8**–**9** (bond lengths in Å, angles in degrees).

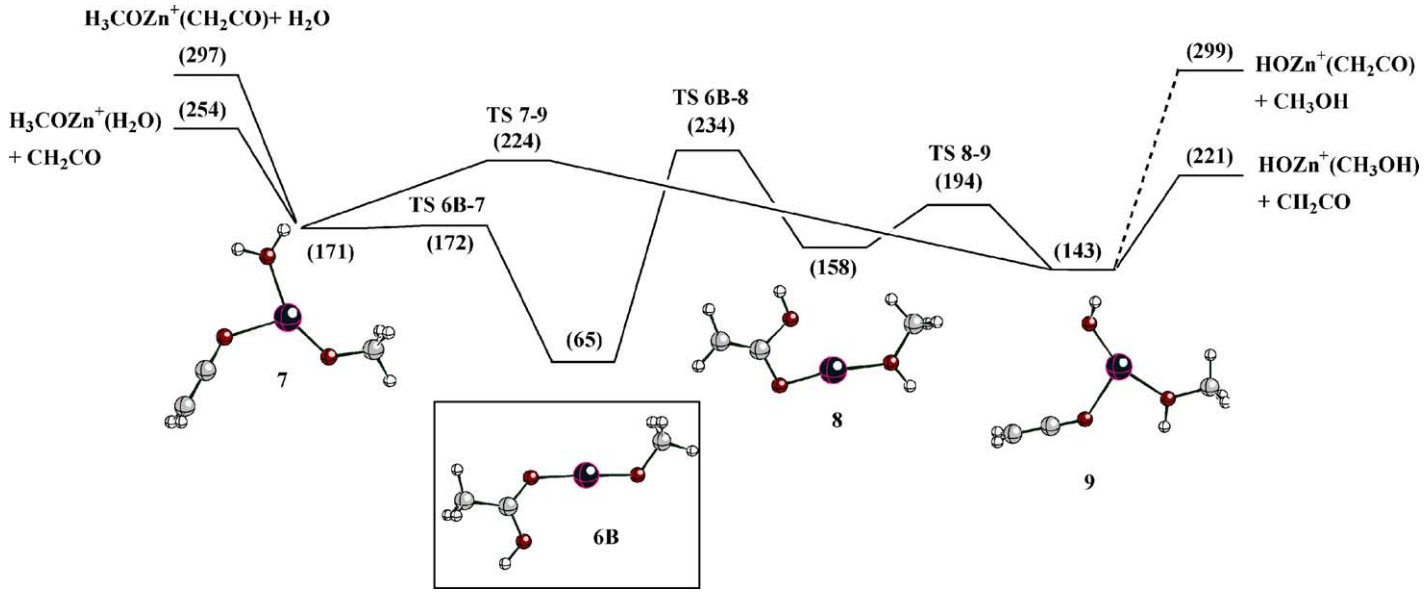

Fig. 10. Potential energy profile of the $[CH_3COOZn, CH_3OH]^+$ system. Elimination of ketene and water. Relative energies (in kJ/mol) are given in parenthesis.

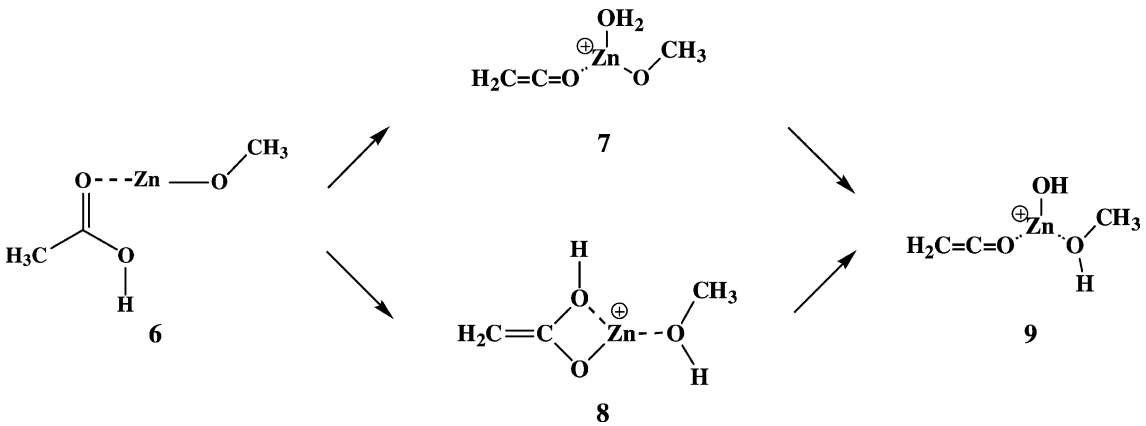

Scheme 2.

at 234 kJ/mol above **5** (Fig. 10), i.e., very close to the transition state TS **7**–**9** (224 kJ/mol above **5**) and to the direct loss of methanol from **5** (239 kJ/mol above **5**). The final state associated with the loss of ketene from **9** is located 221 kJ/mol above **5** (Fig. 10). This loss is in competition with a loss of methanol which is more energy demanding (299 kJ/mol) than the loss of ketene and than the direct desolvation of **5** (239 kJ/mol). However, the hydroxylic hydrogen of the methanol so formed is a non acidic hydrogen and the loss of such a methanol molecule would explain the losses of CH_3OD and CH_3OH from $[CD_3CO_2Zn, CH_3OH]^+$ and $[CH_3CO_2Zn, CH_3OD]^+$, respectively. At last, loss of methanol from **8** may be envisioned. However, the final state associated with this fragmentation ($[CH_2{=}C(OH)OZn + CH_3OH]^+$, 402 kJ/mol above **5**) is too high in energy to be expected.

3.2.5. Summary

The results described above may now be put together to obtain an overall picture of the dissociation of $[CH_3COOZn, CH_3OH]^+$. The most stable isomer of this species is **5**, in which it is the acetic acid ligand which is deprotonated. Direct detachment of the methanol from **5** requires 239 kJ/mol. Isomerisation of **5** into **6A** and **6B** (in which it is the methanol ligand that is deprotonated) opens the way to formation of CH_3CO^+ and elimination of CH_3OZnOH, with a critical energy of 235 kJ/mol. These two major fragmentations have very similar energetic requirements, in agreement with their very similar intensities.

The two minor decomposition pathways, leading to elimination of ketene and water, have critical energies in the same range as the main ones above: 224, 234 and 254 kJ/mol for loss of ketene or higher: 297 kJ/mol for loss of water. These fragmentations as well as the formation of CH_3CO^+ start from **6B**. However, direct formation of CH_3CO^+ is dynamically more favourable than losses of ketene and water because these latter require several successive rearrangements while the former CH_3CO^+ occurs by simple bond cleavage. This is reflected by the small intensities of *m*/*z* 113 (loss of ketene) and *m*/*z* 137 (loss of water) even at high energies. Nevertheless, the loss of water requiring the highest activation energy (comparing with the losses of methanol, $HOZnOCH_3$, CH_2CO) appears at very low collision energy (Fig. 6). As suggested by one reviewer, an interference of a minor isobaric ion evolving from the ESI solvent ($[(H_2O)_5, (CH_3OH)_2, H]^+$) could explain this so early loss.

4. Conclusions

The Zn^{2+}–carboxylate complexes of formic and acetic acids, micro-solvated by a few methanol molecules, undergo methanol evaporation as the lowest energy process. However, when only one methanol

molecule remains on zinc, rearrangement processes become competitive with solvent detachment. In the formate complex, the lowest energy fragmentation is CO_2 loss, triggered by β-H transfer to the metal. It is only at higher energies that direct solvent detachment, being dynamically favoured, becomes the dominant fragmentation. The situation is very different for the acetate complex, in which an analogous β-H transfer does not take place. In this case, there exist rearrangements with critical energies similar to that for methanol detachment. Among these rearrangements, only one (formation of CH_3CO^+) competes with loss of methanol because rearrangement barriers are all very low. The other fragmentations involve rather complex rearrangements which are dynamically disfavoured by high barriers.

The present results provide additional illustrations of the fact that the last desolvation step of the electrospray process is a high energy one, at least for certain types of ions. In such cases, gaseous ions may be chemically different from their precursors in solution. Isomerization within an incompletely desolvated ion is likely to occur if the following conditions are fulfilled: (i) the desolvation of a solvent molecule, particularly the last one, must be energetically demanding. This is most likely to occur in metal-containing ions, and in general when the charge is highly localized; (ii) there must exist rearrangements with low energy barriers; (iii) desolvation from the rearranged structure must be easier than for the parent structure. This is easily achieved if isomerization leads to a species in which the metal charge is reduced or in which the metal coordination sphere is significantly more crowded.

Acknowledgements

This work was supported by a grant of computer time at the Institut de Développement et de Ressources en Informatique Scientifique (IDRIS, project 020543).

References

[1] M. Peschke, A.T. Blades, P. Kebarle, J. Am. Chem. Soc. 122 (2000) 10440.
[2] M. Pavlov, P.E.M. Siegbahn, M. Sandström, J. Phys. Chem. A 102 (1998) 219.
[3] F. Rogalewicz, Y. Hoppilliard, G. Ohanessian, Int. J. Mass Spectrom. 201 (2000) 307.
[4] Y. Hoppilliard, F. Rogalewicz, G. Ohanessian, Int. J. Mass Spectrom. 204 (2001) 267.
[5] F. Rogalewicz, Y. Hoppilliard, G. Ohanessian, Int. J. Mass Spectrom. 206 (2001) 45.
[6] F. Rogalewicz, Y. Hoppilliard, G. Ohanessian, Int. J. Mass Spectrom. 227 (2003) 439.
[7] (a) A.J.H. Wachters, J. Chem. Phys. 52 (1970) 1033;
(b) P.J. Hay, J. Chem. Phys. 66 (1977) 4377.
[8] M.J. Frisch, G.W. Trucks, H.B. Schlegel, G.E. Scuseria, M.A. Robb, J.R. Cheeseman, V.G. Zakrzewski, J.A. Montgomery Jr., R.E. Stratmann, J.C. Burant, S. Dapprich, J.M. Millam, A.D. Daniels, K.N. Kudin, M.C. Strain, O. Farkas, J. Tomasi, V. Barone, M. Cossi, R. Cammi, B. Mennucci, C. Pomelli, C. Adamo, S. Clifford, J. Ochterski, G.A. Petersson, P.Y. Ayala, Q. Cui, K. Morokuma, D.K. Malick, A.D. Rabuck, K. Raghavachari, J.B. Foresman, J. Cioslowski, J.V. Ortiz, B.B. Stefanov, G. Liu, A. Liashenko, P. Piskorz, I. Komaromi, R. Gomperts, R.L. Martin, D.J. Fox, T. Keith, M.A. Al-Laham, C.Y. Peng, A. Nanayakkara, C. Gonzalez, M. Challacombe, P.M.W. Gill, B. Johnson, W. Chen, M.W. Wong, J.L. Andres, C. Gonzalez, M. Head-Gordon, E.S. Replogle, J.A. Pople, Gaussian98 (Revision A.6), Gaussian, Inc., Pittsburgh, PA, 1998.